Polymer Chemistry

ROYAL SOCIETY OF CHEMISTRY

PAPER

View Article Online
View Journal | View Issue

Cite this: *Polym. Chem.*, 2025, **16**, 2389

Cyclic thioacetal carbonates for dual-stimuli degradable poly(vinyl ether)s with cleavable thioacetal and carbonate bonds evenly distributed in the main chains by cationic degenerative chain-transfer copolymerization†

Mineto Uchiyama, * Kaoru Matoba and Masami Kamigaito *

We report the synthesis of dual-stimuli degradable poly(vinyl ether)s with cleavable thioacetal and carbonate bonds evenly distributed in the main chains using cationic degenerative chain-transfer (DT) copolymerization of vinyl ethers with macrocyclic thioacetal carbonates (CTAC). The 22- and 26-membered cyclic thioacetal carbonates (**22-CTAC** and **26-CTAC**) were initially synthesized by a cationic thiol–ene reaction between divinyl ether with a carbonate bond and dithiol with or without a carbonate bond under dilution conditions. These compounds were subjected to cationic copolymerization with vinyl ethers using the HCl-adduct of isobutyl vinyl ether as an initiator and $ZnCl_2$ as a catalyst and were consumed much faster than the vinyl ethers by ring-opening reactions despite the large ring to introduce thioacetal and carbonate bonds in the main chains of the products. The in-chain thioacetal bonds subsequently served as dormant bonds for the cationic DT polymerization of vinyl ethers and enabled the synthesis of poly(vinyl ether)s with controlled total and segmental molecular weights between the thioacetal and carbonate bonds. The orthogonal degradations were successful when acid and base catalysts were used for the thioacetal and carbonate bonds, respectively; this resulted in low-molecular-weight products with controlled molecular weights. Furthermore, multiblock copolymers were synthesized by the one-time addition of the second monomer (B) to the cationic DT polymerization of the first monomer (A) and **22-CTAC** and were selectively degraded into ABA and BAB triblock copolymers with acid and base catalysts, respectively.

Received 16th January 2025,
Accepted 17th April 2025

DOI: 10.1039/d5py00054h

rsc.li/polymers

Introduction

The development of degradable polymer materials is urgently needed since the environmental issues caused by plastic waste have become more severe. In addition to microbial degradation in the natural environment, chemical degradation induced by external stimuli is also useful for developing sustainable polymer materials. Recently, interest in the synthesis of novel polymers with specific bonds that can be cleaved by chemical stimuli has increased.[1–5] These polymers can be chemically degraded and further recycled. Alternatively, chemically degraded low-molecular-weight products can undergo biodegradation naturally, although a rational design of the polymers is needed. Furthermore, more recently, multi-stimuli degradable polymers have attracted increased interest because of their ability to degrade in response to different conditions.[6–8]

Among various synthetic polymers, vinyl polymers have the most significant challenges for degradation because their main chains are composed of stable carbon–carbon single bonds. Several strategies have been developed to increase the degradability or recyclability of vinyl polymers.[9–22] One effective direct approach is the use of heteroatom-containing cyclic monomers that can copolymerize with common vinyl monomers. These cyclic monomers can undergo ring-opening reactions to enable the incorporation of more cleavable carbon–heteroatom bonds in the main chain of the resulting copolymers.[23–51] Alternatively, recent publications have revealed that even acyclic compounds with heteroatoms can be used for the incorporation of heteroatoms in the main chains

Department of Molecular and Macromolecular Chemistry, Graduate School of Engineering, Nagoya University, Furo-cho, Chikusa-ku, Nagoya 464-8603, Japan. E-mail: uchiyama@chembio.nagoya-u.ac.jp, kamigait@chembio.nagoya-u.ac.jp

†Electronic supplementary information (ESI) available: Detailed information on materials, measurements, polymerization and degradation procedures, and additional polymer characterization data (SEC and NMR). See DOI: https://doi.org/10.1039/d5py00054h

via copolymerization with vinyl monomers, as reported in the direct polymerization of carbon–heteroatom double bonds such as C═S and C═O in thiocarbonyl and carbonyl copmpounds[52–57] and isomerization radical polymerizations of specific vinyl ethers accompanying 1,5-shift of atoms and groups.[58–60] In these copolymerization approaches, however, the controlled incorporation of heteroatoms in the main chain is generally difficult except for alternating copolymerization because the comonomers are randomly copolymerized according to the monomer reactivity ratios. Controlled incorporation of carbon–heteroatom bonds is more desirable in terms of regulating the molecular weights of the degraded vinyl oligomer products; these degraded products may further undergo biodegradation.[61–63]

One of the most useful methods to control the molecular weight of the vinyl polymers is "living"/controlled polymerization or reversible deactivation polymerization; here, the dormant polymer terminal functions as a reversibly cleavable bond during the polymerization to enable continuous controlled chain growth. However, dormant bonds are usually located at the polymer terminal. Recently, we developed controlled cationic polymerizations that proceeded *via* reversible activation of the C–S bond *via* degenerative chain transfer (DT) or reversible addition–fragmentation chain transfer (RAFT) of the cationic propagating species to the dormant thioester and thioacetal terminals.[64–80] We also found that thioacetal bonds could be constructed as main-chain linkages of polythioacetals *via* cationic thiol–ene polyaddition of dithiol and divinyl ethers[72,81] or cationic ring-opening polymerization of cyclic thioacetal (CTA).[80] These bonds could be used as in-chain dormant bonds for the subsequent cationic DT polymerization of vinyl ethers, resulting in copolymers with sulfur atoms in the main chain. In particular, a 7-membered cyclic thioacetal (**7-CTA**) efficiently undergoes cationic copolymerization with vinyl ethers through a ring-opening reaction. Here, **7-CTA** is consumed much faster than vinyl ethers and is able to produce mostly polythioacetals in the initial stage. The resulting thioacetal bonds in the main chain serve as in-chain dormant species for the cationic DT polymerization of the remaining vinyl ethers. Thus, vinyl ethers are schematically inserted into the main-chain thioacetal bonds to form the copolymers, in which both the whole and segmental molecular weights of the poly(vinyl ether)s are controlled *via* the DT mechanism. Subsequent treatment of the resulting copolymers with silver nitrate or organic acid solution cleaves the main-chain thioacetals to finally result in poly(vinyl ethers)s with low and controlled molecular weights. Thus, the thioacetal bond in CTA has multiple functions, *i.e.*, a polymerizable group of the cyclic monomer, an in-chain dormant bond for the cationic polymerization of vinyl ethers, and a degradable bond in the resulting vinyl polymers.

In this study, we investigated the synthesis of dual-stimuli degradable poly(vinyl ether)s *via* the incorporation of another degradable bond in CTA and subsequent cationic DT copolymerization with vinyl ethers (Scheme 1). Herein, in addition to the acid-cleavable thioacetal bond, carbonate was chosen as the other degradable bond, and could be cleaved under basic conditions, thus enabling dual-stimuli degradation. Novel macrocyclic thioacetals with carbonate bonds were synthesized by a cationic thiol–ene reaction between divinyl ether with a carbonate bond and dithiol with or without a carbonate bond under dilution conditions. The obtained macrocyclic thioace-

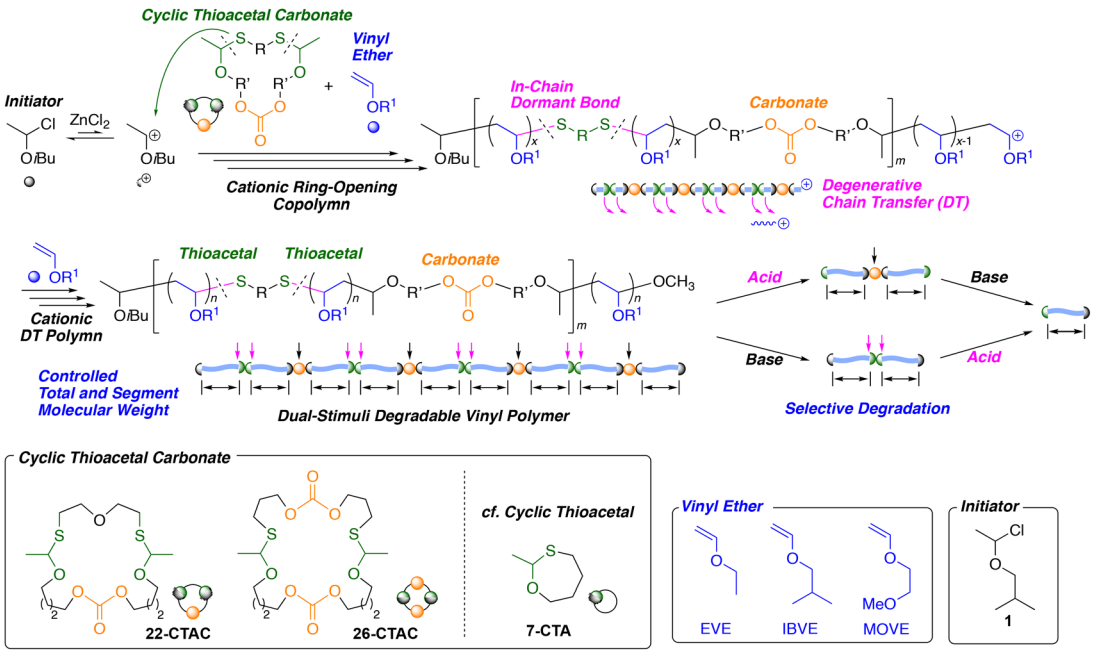

Scheme 1 Synthesis and selective degradation of poly(vinyl ether)s with periodically distributed thioacetal and carbonate bonds in main chains by cationic degenerative chain-transfer copolymerization of vinyl ethers and cyclic thioacetal carbonate.

tal carbonate was used as a comonomer and a precursor for the in-chain dormant species in the cationic copolymerization with vinyl ethers. In this case, the carbonate bond could be introduced into the main chains along with the thioacetal bond *via* the ring-opening reaction of the macrocyclic thioacetal carbonate. The cationic DT polymerization of vinyl ethers based on the in-chain thioacetal bonds enabled the formation of poly(vinyl ether)s with controlled segment lengths, which were linked with both thioacetal and carbonate bonds. The orthogonal degradation of the obtained copolymers was investigated using acid and base catalysts for the cleavage of thioacetal and carbonate bonds, respectively. Furthermore, the one-pot synthesis of multiblock copolymers with dual degradability was also investigated.

Results and discussion

Synthesis of macrocyclic thioacetal carbonate

Macrocyclic thioacetal carbonates were synthesized by a cationic thiol–ene reaction between a divinyl ether with a carbonate group and a dithiol with or without a carbonate group using benzenesulfonic acid (BSA) as an acid catalyst under dilution conditions (Scheme 2).[81]

The synthesis of a 22-membered cyclic thioacetal carbonate (**22-CTAC**) with one carbonate and two thioacetal bonds is first described (Scheme S1†). A symmetrical divinyl ether with a carbonate group, *i.e.*, bis[4-(vinyloxy)butyl]carbonate (**DVE-1**), was prepared by the reaction between 4-hydroxybutyl vinyl ether and 1,1′-carbonyldiimdazole. A dithiol, bis(2-mercaptoethyl)ether (**DT-1**), was commercially available. Then, the cationic thiol–ene reaction between **DVE-1** and **DT-1** was examined with equimolar amounts under dilution conditions ($[\mathbf{DVE\text{-}1}]_0/[\mathbf{DT\text{-}1}]_0$ = 25/25 mM) in the presence of a catalytic amount of BSA ($[BSA]_0$ = 0.10 mM) in CH_2Cl_2 at −40 °C. Both thiol and vinyl ether were quantitatively consumed. The peak-top molecular weight (M_p) of the size-exclusion chromatography (SEC) curve of the main product was 340; this result indicated the formation of a 1 : 1 adduct (Fig. 1A). After purification by silica column chromatography, the SEC curve became monomodal. In addition, the ^{1}H NMR spectrum

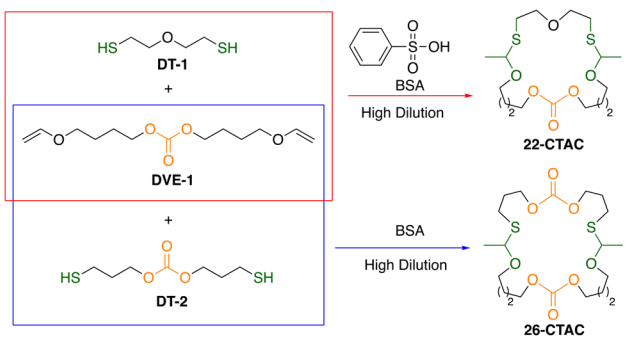

Scheme 2 Synthesis of cyclic thioacetal carbonate by cationic thiol–ene reaction between divinyl ether with carbonate linkage and dithiol.

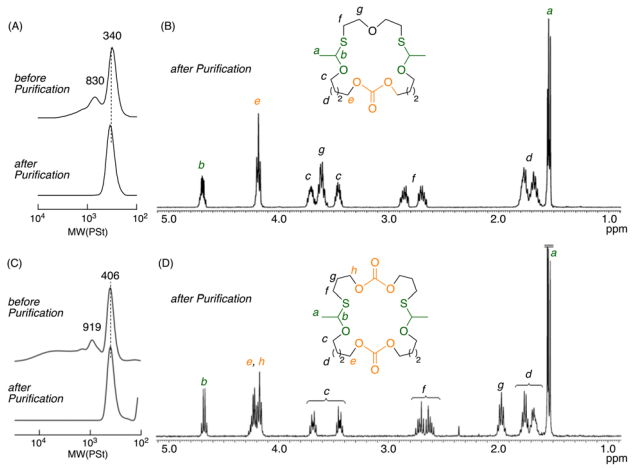

Fig. 1 SEC curves (A and C) and ^{1}H NMR spectra ($CDCl_3$, r.t.) (B and D) of **22-CTAC** (for A and B) and **26-CTAC** (C and D) obtained by cationic thiol–ene reaction of **DVE-1** and dithiols under dilute conditions: $[\mathbf{DVE\text{-}1}]_0/[\mathbf{DT\text{-}1}]_0/[BSA]_0$ = 25/25/0.10 mM or $[\mathbf{DVE\text{-}1}]_0/[\mathbf{DT\text{-}2}]_0/[BSA]_0$ = 50/50/0.20 mM in CH_2Cl_2 at −40 °C.

showed characteristic peaks; these peaks were attributed to thioacetal (*b*) and carbonate (*e*) groups and were present at a 2 : 1 ratio (Fig. 1B). In addition, the MALDI-TOF-MS spectrum also confirmed that the main product was the desired 1 : 1 adduct (Fig. S3†). Thus, a 22-membered cyclic thioacetal carbonate (**22-CTAC**) with two thioacetal bonds and one carbonate bond was successfully synthesized.

Another cyclic thioacetal carbonate (**26-CTAC**) with a 26-membered ring linked by two carbonate and two thioacetal bonds was also prepared by a similar cationic thiol–ene reaction involving an equimolar mixture of **DVE-1** and bis(3-mecaptopropyl)carbonate (**DT-2**); **DT-2** was prepared from bis(3-choloropropyl)carbonate and potassium thioacetate followed by deacetylation (Scheme S2†). In this case, both divinyl ether (**DVE-1**) and dithiol (**DT-2**) possess a carbonate bond. Although slightly higher amounts of high-molecular-weight products were observed in the SEC curve of the products, the main product with an M_p of 406 was purified by column chromatography (Fig. 1C). The ^{1}H NMR spectrum showed two kinds of carbonate peaks (*e* and *h*) and one thioacetal peak (*b*) with a peak area ratio of $(e + h) : b = 4 : 1$ (Fig. 1D); these results indicated that this molecule had two different carbonate bonds and two identical thioacetal bonds. The formation of macrocyclic 26-membered cyclic thioacetal carbonate was also supported by the MALDI-TOF-MS spectrum (Fig. S8†).

22-Membered cyclic thioacetal carbonate for cationic DT copolymerization with ethyl vinyl ether

Cationic copolymerization of ethyl vinyl ether (EVE) and **22-CTAC** was investigated with the HCl adduct of isobutyl vinyl ether (**1**) as an initiator and $ZnCl_2$ as a catalyst in a similar way to the copolymerization of EVE and **7-CTA**.[80] Fig. 2 shows representative results for the copolymerization in the mixture of CH_2Cl_2, toluene, and Et_2O (80/10/10) at −40 °C, where the

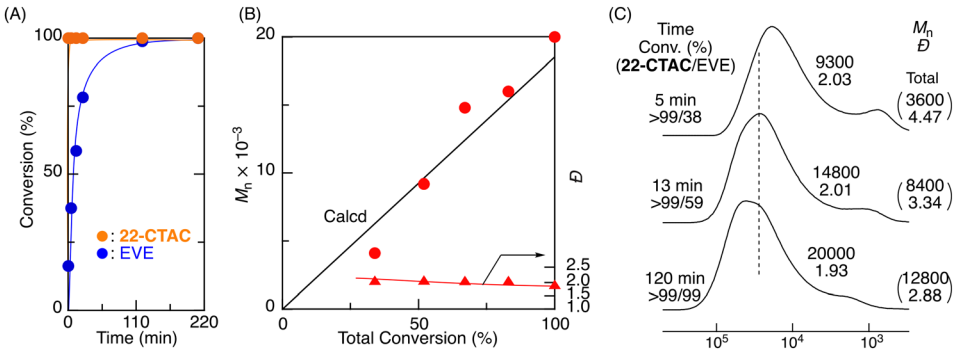

Fig. 2 Time-conversion curve (A), M_n values (B), and SEC curves (C) of the polymers obtained in cationic DT copolymerization of EVE and **22-CTAC**: $[EVE]_0/[\textbf{22-CTAC}]_0/[\textbf{1}]_0/[ZnCl_2]_0$ = 4000/200/20/4.0 mM in CH_2Cl_2/*n*-hexane/Et_2O (20/10/10) at −40 °C.

feed ratios of the monomers (EVE + **22-CTAC**) to the initiator (**1**) and EVE to **22-CTAC** were 200 + 10 and 20, respectively ($[EVE]_0/[\textbf{22-CTAC}]_0/[\textbf{1}]_0$ = 4000/200/20 mM). The cyclic thioacetal carbonate was consumed more rapidly than EVE, irrespective of the large ring, and both monomers were quantitatively consumed (Fig. 2A). In the SEC curves, two peaks were present, and both shifted to the high-molecular-weight regions along with the consumption of EVE (Fig. 2B). As the polymerization proceeded, the lower-molecular-weight peak was attributed to the cyclic oligomers formed *via* the intramolecular DT reaction and decreased.[80] The number-average molecular weight (M_n) of the main peak linearly increased with monomer conversion and was in good agreement with the theoretical values, assuming that one copolymer chain was generated from one molecule of **1** (Fig. 2B). However, the dispersities ($Đ$) were relatively broad during the polymerization. This was attributed to the shuffling of poly(EVE) segments among the polymer chains because the growing carbocationic species could attack the in-chain dormant thioacetal bonds to induce reversible main-chain cleavage *via* the DT mechanism. These results were similar to those obtained with **7-CTA**, as reported previously.[80] Thus, despite the larger ring size, the 22-membered macrocyclic thioacetal carbonate, *i.e.*, **22-CTAC**, successfully underwent cationic DT copolymerization with EVE.

Then, the final product was purified to remove the lower-molecular-weight oligomers using preparative SEC to produce the isolated main product (M_n = 17 900, $Đ$ = 2.20), and this product was then analyzed by ^{1}H NMR spectroscopy. The characteristic peaks derived from the ring-opened structure of **22-CTAC** were the methine proton of the thioacetal at 4.7 ppm (*e*), the methylene proton next to the sulfur atom at 2.7 ppm (*f*), and the methylene proton (*l*) next to the carbonate group at 4.1 ppm; these peaks were observed in addition to the large peaks of the poly(EVE) segments (Fig. 3A). These results indicated that the thioacetal and carbonate bonds derived from **22-CTAC** were incorporated into the poly(EVE) main chains *via* a ring-opening reaction.

Furthermore, additional small peaks were present and attributed to the terminal protons, such as the methyl proton (α_2) of the isobutyl group at the α-chain end derived from the initiator at 0.9 ppm and the methine proton (ω_1) of the acetal at the ω-chain end generated *via* termination reaction with methanol at 4.6 ppm; this peak overlapped with the methine proton of the main-chain thioacetal (*e*). The average number ($2m$) of the incorporated thioacetal bonds calculated from the integral ratio of f to α_2 was 18. Additionally, the average number (m) of the incorporated carbonate bonds calculated from the integral ratio of l to α_2 was 9; this value was in agreement with half the number of thioacetal bonds. These numbers were close to the theoretical values calculated from the feed ratio of **22-CTAC** to **1** ($[\textbf{22-CTAC}]_0/[\textbf{1}]_0$ = 10); these results indicated that **22-CTAC** was quantitatively incorporated into the polymer main chains. Moreover, the number-average degree (n) of poly(EVE) segments per thioacetal bond was calculated from the integral ratio of EVE units to the sum of in-chain thioacetal and terminal acetal bonds and was determined to be 10. These results indicated that the obtained copolymer was composed of 19 (= $2m$ + 1) poly(EVE) segments with 10 (= n) EVE units on average and contained 18 (= $2m$) thioacetal bonds and 9 (= m) carbonate bonds in the main chain.

Degradation of the copolymer

The thioacetal and carbonate bonds in the polymer main chains could be selectively cleaved by different stimuli or catalysts. The selective degradation of the obtained copolymers was investigated using different catalysts. The degradation *via* hydrolysis of the thioacetal bonds was initially examined using an $AgNO_3$ solution in a mixture of THF and H_2O at room temperature.[80,82–85] After 3 h, the SEC curve of the products shifted to the low-molecular-weight region (Fig. 4A). The M_n value decreased to 2200 and was in agreement with the calculated value (2000), assuming that one thioacetal bond formed one poly(EVE) segment. In addition, the dispersity of the degraded products decreased ($Đ$ = 1.27). The ^{1}H NMR spectrum of the resulting products revealed that the peak (*e*) derived from the thioacetal bond at 4.6 ppm completely disappeared and that a new peak (*x*) attributed to the aldehyde terminal was formed *via* hydrolysis and appeared at 9.8 ppm

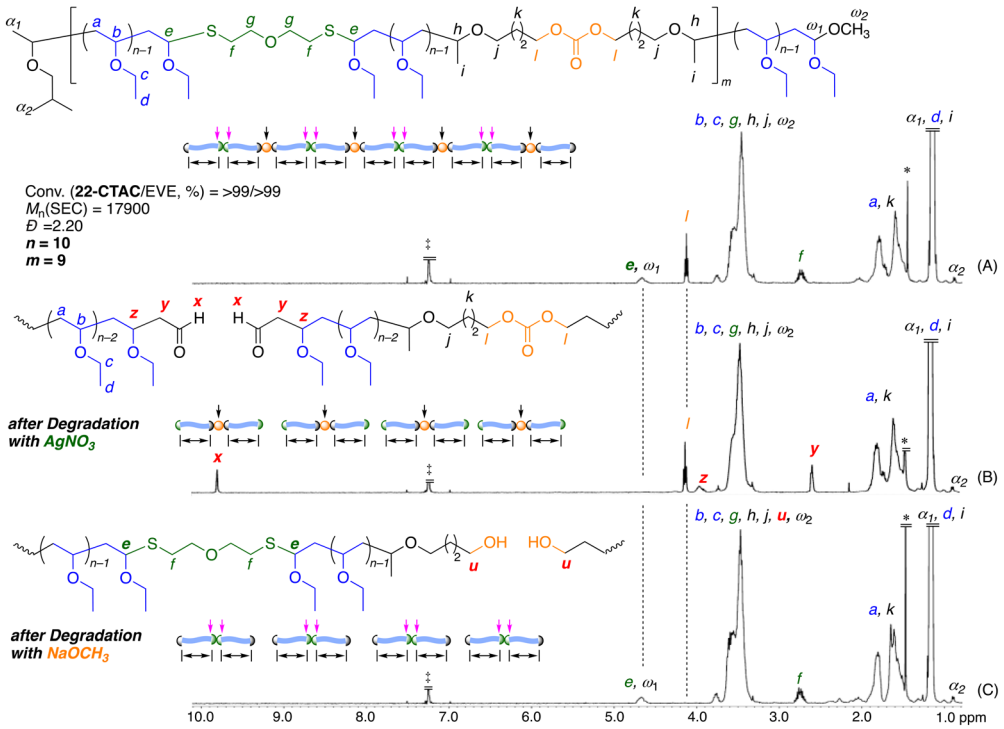

Fig. 3 ^{1}H NMR spectra ($CDCl_3$, 55 °C) of the obtained copolymer of EVE and **22-CTAC** (A) and the polymers after degradation using an $AgNO_3$ solution (B) and using a $NaOCH_3$ solution (C): [thioacetal unit]$_0$/[$AgNO_3$]$_0$ = 5.0/50 mM in THF/H_2O at 20 °C or [carbonate unit]$_0$/[$NaOCH_3$]$_0$ = 5.0/50 mM in CH_3OH at 60 °C. *: H_2O, ‡: $CHCl_3$.

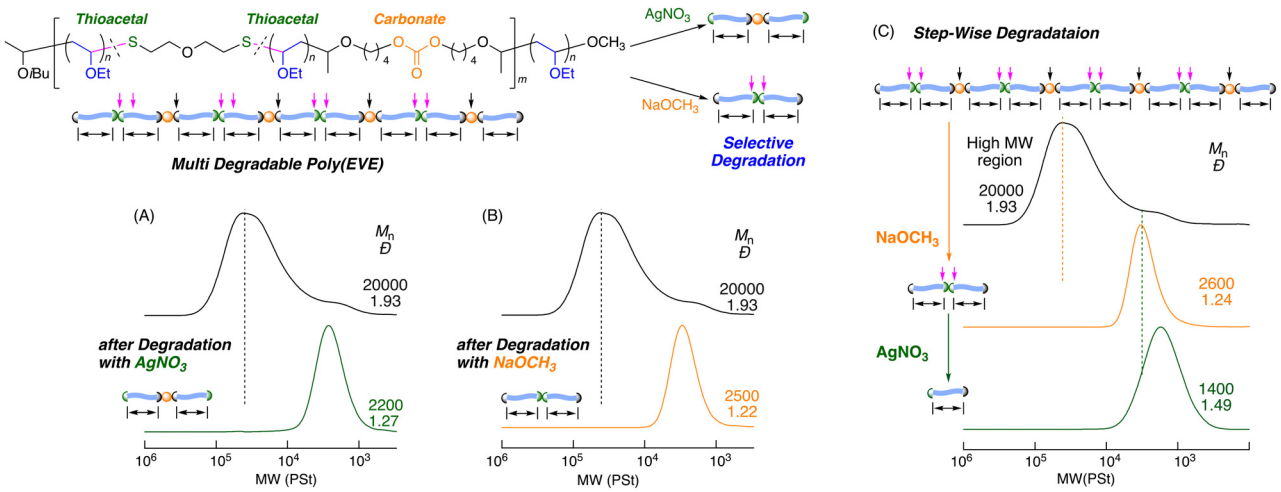

Fig. 4 SEC curves of the products before and after degradation with $AgNO_3$ (A) and $NaOCH_3$ (B), and SEC curves of the products obtained by dual degradation with the sequential use of $NaOCH_3$ and $AgNO_3$ (C): [thioacetal unit]$_0$/[$AgNO_3$]$_0$ = 5.0/50 mM in THF/H_2O at 20 °C. [Carbonate]$_0$/[$NaOCH_3$]$_0$ = 5.0/50 mM in CH_3OH at 60 °C.

(Fig. 3B). Furthermore, the peaks derived from carbonate bonds remained unchanged after treatment with the $AgNO_3$ solution. These results indicated that the thioacetal bonds were evenly distributed in the main chain of the obtained copolymers and that they were selectively cleaved by $AgNO_3$. A similar selective cleavage of the thioacetal bonds was also examined using a common organic acid such as *p*-toluenesulfonic acid. The degradation was slower, but the selective degradation was supported by the SEC and ^{1}H NMR analyses (Fig. S9 and S10†).

The selective degradation of the carbonate bonds was then investigated *via* methanolysis using a $NaOCH_3$ solution in CH_3OH at 60 °C. The SEC curve of the products obtained after 48 h shifted to the low-molecular-weight region (M_n = 2500) and

became narrow ($Đ$ = 1.23) (Fig. 4B), as in the case of $AgNO_3$. More interestingly, peak (l) of the methylene proton adjacent to the carbonate groups completely disappeared, whereas peak (e) attributed to the thioacetal bonds remained intact (Fig. 3C). These results indicated that selective complementary degradation occurred when the base catalyst was used in place of the acid catalyst. The degradations were thus orthogonal. Additionally, kinetic comparison under these specific conditions revealed that degradation of carbonate bonds with $NaOCH_3$ proceeded much slower than that of thioacetal bonds with $AgNO_3$. The degradation progress with $NaOCH_3$ was examined by SEC and ^{1}H NMR (Fig. S11 and S12†). As shown in Fig. S12,† the M_n values of the products were measured by SEC and decreased with increasing degradation of the carbonate moiety, as measured by ^{1}H NMR (Fig. S11†). The plots were effectively fit with the theoretical curves, assuming that the carbonate bonds were evenly incorporated into the main chains of the copolymers.

Based on these results, stepwise degradation was investigated using a base catalyst followed by an acid catalyst. The first degradation using the $NaOCH_3$ solution resulted in a low-molecular-weight polymer with a narrow dispersity (M_n = 2600, $Đ$ = 1.24) (Fig. 4C). The recovered polymer with thioacetal bonds was subsequently subjected to a second degradation using the $AgNO_3$ solution. The SEC curve further shifted to the low-molecular-weight region; this resulted in a product with M_n = 1400, which was reduced by approximately half of the first degraded products. These results indicated that the thioacetal bonds were located around the middle of the first degradation products and that dual-stimuli degradable poly(EVE) with thioacetal and carbonate bonds, which were evenly distributed in the main chain, was obtained by the cationic DT copolymerization of EVE and **22-CTAC**.

Tunable molecular weights before and after degradation

In this copolymerization, the overall molecular weights of the products before degradation could be controlled by the feed ratio of total monomers to initiator, whereas the molecular weights of the degraded products could be controlled by the feed ratio of vinyl ether to cyclic thioacetal.[80]

Here, the control of the total molecular weight of the copolymer was investigated by changing the feed ratio of the total monomers to the initiator ($([EVE]_0 + [\mathbf{22\text{-}CTAC}]_0)/[\mathbf{1}]_0$ = 100 + 5, 200 + 10, and 400 + 20), while the feed ratio of vinyl ether to cyclic thioacetal carbonate was fixed ($[EVE]_0/[\mathbf{22\text{-}CTAC}]_0$ = 20). This enabled the synthesis of polymers with different overall molecular weights while maintaining the same molecular weights of the degraded products. In all cases, **22-CTAC** was consumed much faster than EVE (Fig. S13†), resulting in copolymers (Fig. S14†). The M_n values of the products varied with the feed ratio of total monomers to initiator (M_n = 10 000–40 000) and effectively agreed with the theoretical values, assuming that one initiator generates one polymer chain (Fig. 5A).

The selective degradation of a series of copolymers with different total molecular weights was examined similarly using $AgNO_3$ and $NaOCH_3$ solutions. In all cases, the SEC curves shifted to the low-molecular-weight region and became narrower ($Đ$ = 1.2–1.3) (Fig. 5B and C). Despite the different original molecular weights and different stimuli used, the M_p and M_n after degradation were nearly the same (M_n ~ 2000) and agreed well with theoretical values. Thus, this method enabled the synthesis of a series of dual-stimuli degradable polymers; these polymers had overall different molecular weights tunable by the varied feed ratios of monomers and initiators but could be degraded into the same molecular weights determined by the fixed feed ratio of vinyl ether to cyclic thioacetal carbonate.

Next, the control of the molecular weights of the degraded products was examined by varying the concentration of cyclic thioacetal carbonate without changing the concentrations of the vinyl ether and initiator. The feed ratio of EVE to **22-CTAC** was varied from 10 to 20 and 40 ($[EVE]_0/[\mathbf{22\text{-}CTAC}]_0$ = 10, 20, and 40), whereas that of EVE to **1** was kept constant at 200 ($[EVE]_0/[\mathbf{1}]_0$ = 200). The consumption of **22-CTAC** was much

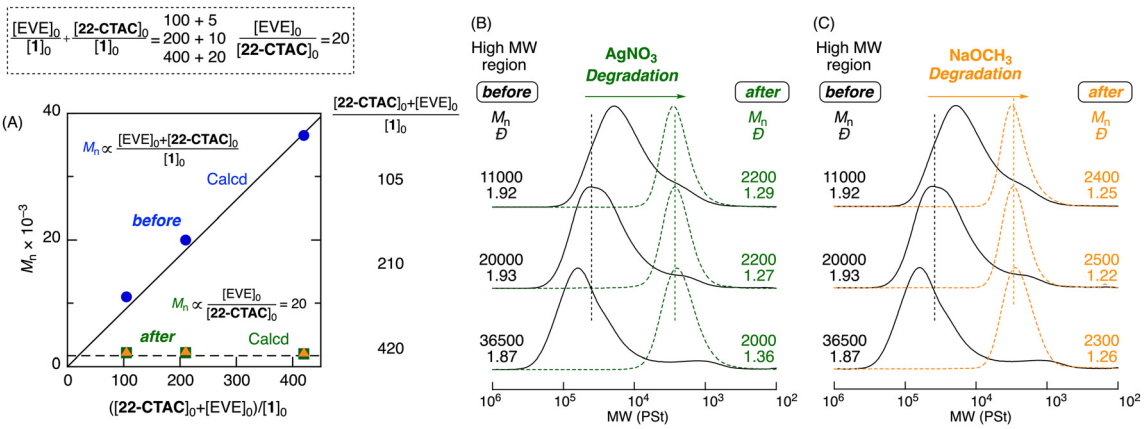

Fig. 5 Effect of varying $([EVE]_0 + [\mathbf{22\text{-}CTAC}]_0)/[\mathbf{1}]_0$ with constant $[EVE]_0/[\mathbf{22\text{-}CTAC}]_0$ on M_n values (A) and SEC curves (B and C) of the polymers obtained by cationic DT copolymerizations of EVE and **22-CTAC** before and after degradation: $[EVE]_0/[\mathbf{22\text{-}CTAC}]_0/[\mathbf{1}]_0/[ZnCl_2]_0$ = 4000/200/10, 20, 40/4.0 mM in CH_2Cl_2/*n*-hexane/Et_2O (20/10/10) at −40 °C. [Thioacetal unit]$_0$/$[AgNO_3]_0$ = 5.0/50 mM in THF/H_2O at 20 °C. [Carbonate]$_0$/$[NaOCH_3]_0$ = 5.0/50 mM in CH_3OH at 60 °C.

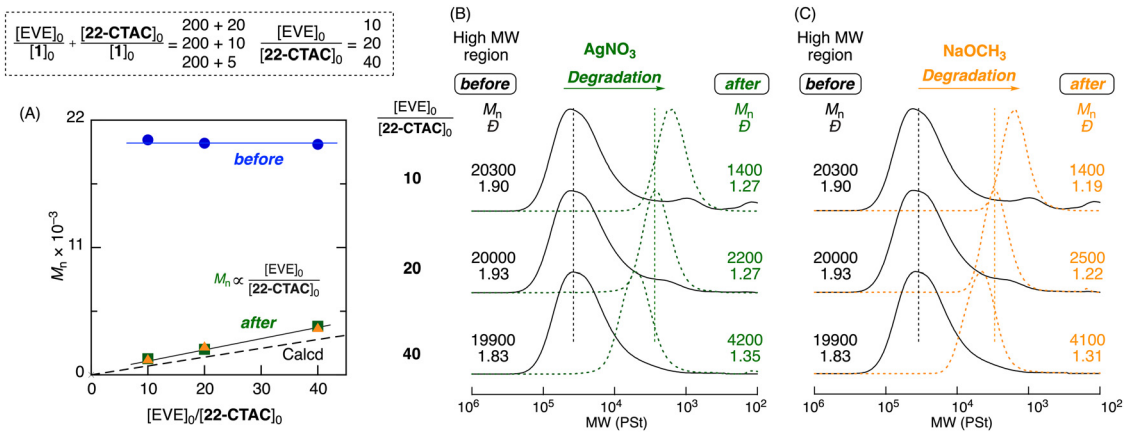

Fig. 6 Effect of varying $[EVE]_0/[\textbf{22-CTAC}]_0$ with constant $[EVE]_0/[\textbf{1}]_0$ on M_n values and SEC curves (B and C) of the polymers obtained by cationic DT copolymerizations of EVE and **22-CTAC** before and after degradation: $[EVE]_0/[\textbf{22-CTAC}]_0/[\textbf{1}]_0/[ZnCl_2]_0$ = 4000/100, 200, 400/20/4.0 mM in CH_2Cl_2/*n*-hexane/Et_2O (20/10/10) at −40 °C. $[Thioacetal\ unit]_0/[AgNO_3]_0$ = 5.0/50 mM in THF/H_2O at 20 °C. $[Carbonate]_0/[NaOCH_3]_0$ = 5.0/50 mM in CH_3OH at 60 °C.

faster than that of EVE in all cases (Fig. S15†), resulting in copolymers (Fig. S16†). The SEC analysis of the products revealed that the molecular weights of the obtained copolymers were nearly constant ($M_n \sim 20\,000$) (Fig. 6A).

$AgNO_3$ and $NaOCH_3$ were then similarly used for selective degradation. All SEC curves of the degraded products shifted to low-molecular-weight regions with decreasing dispersity (Fig. 6B and C). Here, the shifts became more remarkable as the **22-CTAC** feed increased, and they were nearly independent of the catalysts ($AgNO_3$ and $NaOCH_3$) used for degradation. Furthermore, the M_n values of the degraded products were close to the theoretical values in which one thioacetal bond generated one poly(EVE) segment and linearly increased with the feed ratio of EVE to **22-CTAC**. Thus, another series of dual-stimuli degradable polymers, with the same molecular weights determined by the fixed feed ratio of vinyl ether to initiator, could be degraded into different molecular weights that were tunable by the varied feed ratios of vinyl ether to cyclic thioacetal carbonate.

These results indicated that dual-stimuli degradable polymers with tunable molecular weights before and after degradation could be synthesized by cationic DT copolymerization of vinyl ether and macrocyclic thioacetal carbonate, which has two thioacetal bonds and one carbonate bond.

Effect of cyclic thioacetal carbonate: 26-CTAC *vs.* 22-CTAC

The other macrocyclic thioacetal carbonate (**26-CTAC**) with two carbonate and two thioacetal bonds in a larger ring was similarly copolymerized with EVE to synthesize another series of dual-stimuli degradable poly(EVE). In contrast to **22-CTAC**, **26-CTAC** possesses another carbonate bond originating from the dithiol unit (**DT-2**) as the starting material in addition to the other carbonate bond originating from the divinyl ether unit (**DVE-1**). Consequently, the base-induced degradation of the polymers produced from **26-CTAC** could reduce the molecular weight of the degraded products to half of that of those from **22-CTAC**.

The cationic DT copolymerization of **26-CTAC** and EVE was similarly examined using the **1**/$ZnCl_2$ system. The consumption of **26-CTAC** occurred more rapidly than that of EVE (Fig. 7A), as in the case of **22-CTAC**. The SEC curves shifted to high-molecular-weight regions as the polymerization proceeded (Fig. 7B). The M_n of the main peak increased in direct proportion to monomer conversion and was similar to the calculated value (Fig. S17†). The ^1H NMR spectrum of the main-peak products purified by preparative SEC revealed two kinds of carbonate bonds and one kind of thioacetal bond originating from **26-CTAC** (Fig. S18A†). The average numbers of the incorporated thioacetal bonds ($2m$) and carbonate bonds ($2m$) calculated from the respective peak area ratios were both 16. The number-average degree (n) of poly(EVE) segments per thioacetal or carbonate bond was 10 (Fig. S18A†). These values were similar to the theoretical values determined by the feed ratios. Thus, **26-CTAC** similarly underwent cationic ring-opening copolymerization with EVE to produce polymers with twice the number of carbonate bonds in the polymer chains as those obtained with **22-CTAC**.

The selective degradation of the thioacetal and carbonate bonds was then investigated using $AgNO_3$ and $NaOCH_3$ solutions, respectively. In both cases, the SEC curves of the products shifted to the low-molecular-weight region and became narrower (Fig. 7C). In particular, the M_n value after degradation with $NaOCH_3$ was reduced to approximately half of that obtained with $AgNO_3$. This result was consistent with the designed polymer structure and indicated that the dual-stimuli degradable poly(vinyl ether)s were rationally designed on the basis of the structure of the macrocyclic thioacetal carbonates.

Various vinyl ethers for cationic copolymerization with 22-CTAC

To adapt the dual-stimuli degradable poly(vinyl ether)s, other vinyl ethers, such as isobutyl (IBVE) and 2-methoxyethyl vinyl ether (MOVE), which are typical hydrophobic and hydrophilic

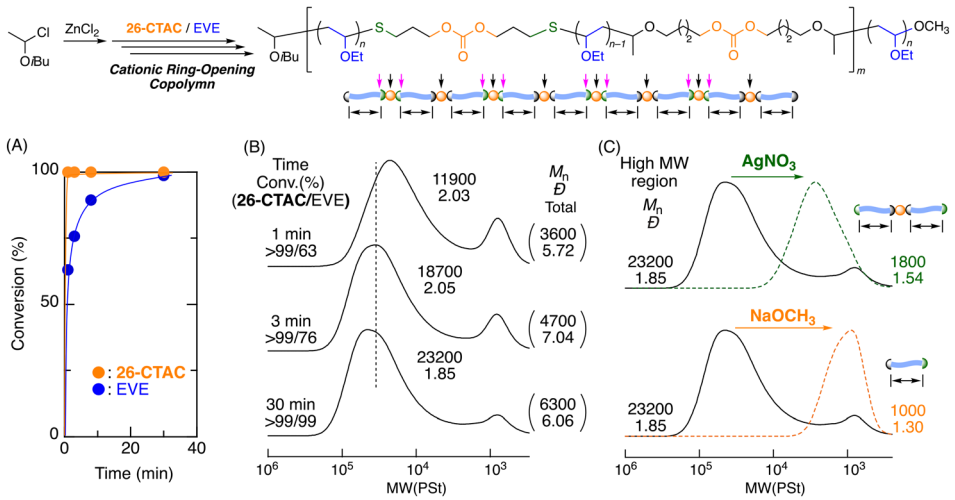

Fig. 7 Time-conversion curve (A) and SEC curves of the polymers obtained in cationic DT copolymerization of EVE with **26-CTAC** before (B) and after (C) degradation with $AgNO_3$ and $NaOCH_3$: $[EVE]_0/[\mathbf{26\text{-}CTAC}]_0/[\mathbf{1}]_0/[ZnCl_2]_0$ = 4000/200/20/8.0 mM in CH_2Cl_2/*n*-hexane/Et_2O (20/10/10) at −40 °C. $[Thioacetal\ unit]_0/[AgNO_3]_0$ = 5.0/50 mM in THF/H_2O at 20 °C. $[Carbonate]_0/[NaOCH_3]_0$ = 5.0/50 mM in CH_3OH at 60 °C.

monomers widely used in cationic polymerizations, were copolymerized with **22-CTAC**. As in the case of EVE, IBVE and MOVE were nearly quantitatively consumed after rapid consumption of **22-CTAC** (Fig. 8). In both cases, the M_n values of the obtained copolymers increased in direct proportion to monomer conversion and were similar to the theoretical values (Fig. S20 and S21†). The M_n of the final products reached 20 000 in this case.

The obtained copolymers were also analyzed by ^1H NMR. The broad large peaks were attributed to each vinyl ether unit and relatively sharp peaks derived from the ring-opened **22-CTAC** units (Fig. S22 and S23†). The average numbers of thioacetal ($2m$) and carbonate bonds (m) in each copolymer were 18 and 9 for IBVE and 20 and 10 for MOVE, respectively. In addition, the number-average degrees (n) of the poly(IBVE) and poly(MOVE) segments were 10 and 14, respectively, and were similar to the theoretical values based on the feed ratio of the monomers to the initiator. Thus, these vinyl ethers were also successfully copolymerized with **22-CTAC**.

The obtained copolymers were then subjected to stepwise degradation using $NaOCH_3$ and $AgNO_3$ sequentially. In both cases, the first reaction with $NaOCH_3$ significantly shifted the SEC curves to low-molecular-weight regions, where the M_n values of the products decreased to approximately 2000 and became narrower (Fig. 8). The second reaction with $AgNO_3$ resulted in M_n values approximately half those of the first products. Thus, cyclic thioacetal carbonates could be widely used for the synthesis of various dual-stimuli degradable poly(vinyl ether)s with different side chains.

Multiblock copolymers with dual-stimuli degradability

Finally, the one-pot synthesis of dual-stimuli degradable multiblock poly(vinyl ether)s was investigated *via* the only one-time addition of a second monomer (B) to the copolymerization of

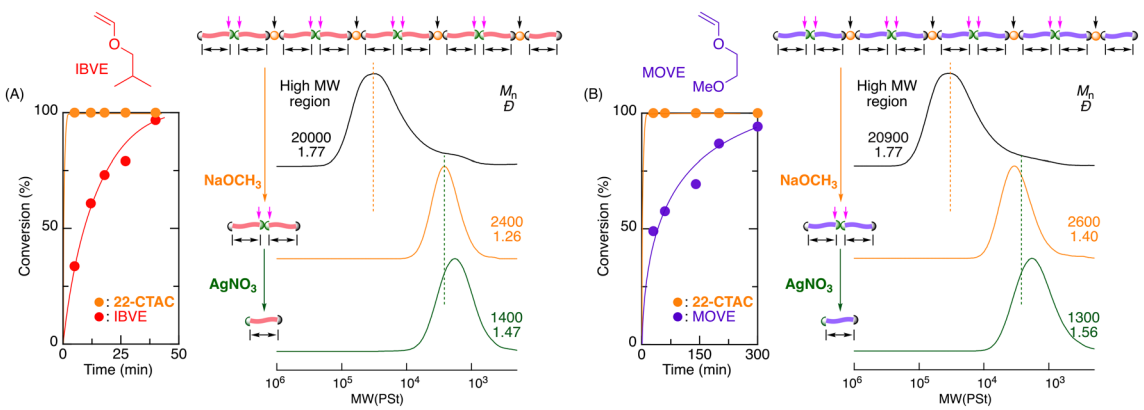

Fig. 8 Cationic DT copolymerization of IBVE (A) and MOVE (B) with **22-CTAC** and SEC curves before and after stepwise degradation: $[VE]_0/[\mathbf{22\text{-}CTAC}]_0/[\mathbf{1}]_0/[ZnCl_2]_0$ = 4000/200/20/4.0 mM in CH_2Cl_2/*n*-hexane/Et_2O (20/10/10) at −40 °C. $[Thioacetal\ unit]_0/[AgNO_3]_0$ = 5.0/50 mM in THF/H_2O at 20 °C. $[Carbonate]_0/[NaOCH_3]_0$ = 5.0/50 mM in CH_3OH at 60 °C.

the first vinyl ether (A) and **22-CTAC**. Herein, the main-chain thioacetal bond formed in the first copolymerization works as the in-chain dormant bond, into which the second monomer was schematically inserted to form the AB diblock copolymer segments connected by both thioacetal and carbonate bonds. Moreover, as shown in the scheme in Fig. 9, the carbonate bond should be located in the middle of the first segment (poly(A)), whereas the two thioacetal bonds should be located in the middle of the second segment (poly(B)). The selective degradation of the copolymers using $AgNO_3$ and $NaOCH_3$ should result in different triblock copolymers, *i.e.*, ABA and BAB copolymers, respectively.

To demonstrate this feasibility, IBVE was chosen as the first monomer (A) and copolymerized with **22-CTAC** using the **1**/$ZnCl_2$ initiating system. After quantitative consumption of IBVE, EVE was added to the reaction solution as the second monomer (B) and was also smoothly consumed (Fig. S26†). After the addition of EVE, the SEC curves (black solid lines in Fig. 9) shifted to the high-molecular-weight regions; these results indicated that EVE was copolymerized into the main-chain thioacetal of the poly(IBVE) segments to form the block copolymer segments. The ^{1}H NMR analysis further supported the formation of block copolymers since the peaks attributed to both EVE and IBVE units were observed in addition to the peaks derived from the ring-opened **22-CTAC** unit (Fig. S27†). The number-average degrees of poly(IBVE) and poly(EVE) segments were calculated from the integral ratios of each peak and were both 8, and the average number of thioacetal groups ($2m$) in the main chain was 11. These results showed the formation of the multiblock copolymer, in which 11 block copolymer segments with 8 IBVE and EVE units on average were connected with thioacetal and carbonate bonds.

The selective degradations of the first polymer and the multiblock copolymer were also investigated using $AgNO_3$ and $NaOCH_3$ separately. In the case of $AgNO_3$, both SEC curves of the products shifted to low-molecular-weight regions (green dashed lines) and became narrower (Fig. 9A). In particular, the SEC curve obtained from the multiblock copolymer was located in higher-molecular-weight regions than that obtained from the first polymer. Similar results were obtained for $NaOCH_3$ (orange dashed lines). Furthermore, the M_n values of the degraded products were independent of the catalyst. The ^{1}H NMR analysis also supported the selective degradation reactions. The peak derived from the thioacetal groups disappeared with $AgNO_3$ along with the appearance of aldehyde terminals, whereas the peak of the methylene protons adjacent to the carbonate group disappeared with $NaOCH_3$ (Fig. S28†). In contrast, the carbonate and thioacetal groups remained unchanged with $AgNO_3$ and $NaOCH_3$, respectively. Thus, the products degraded with $AgNO_3$ were ABA triblock polymers

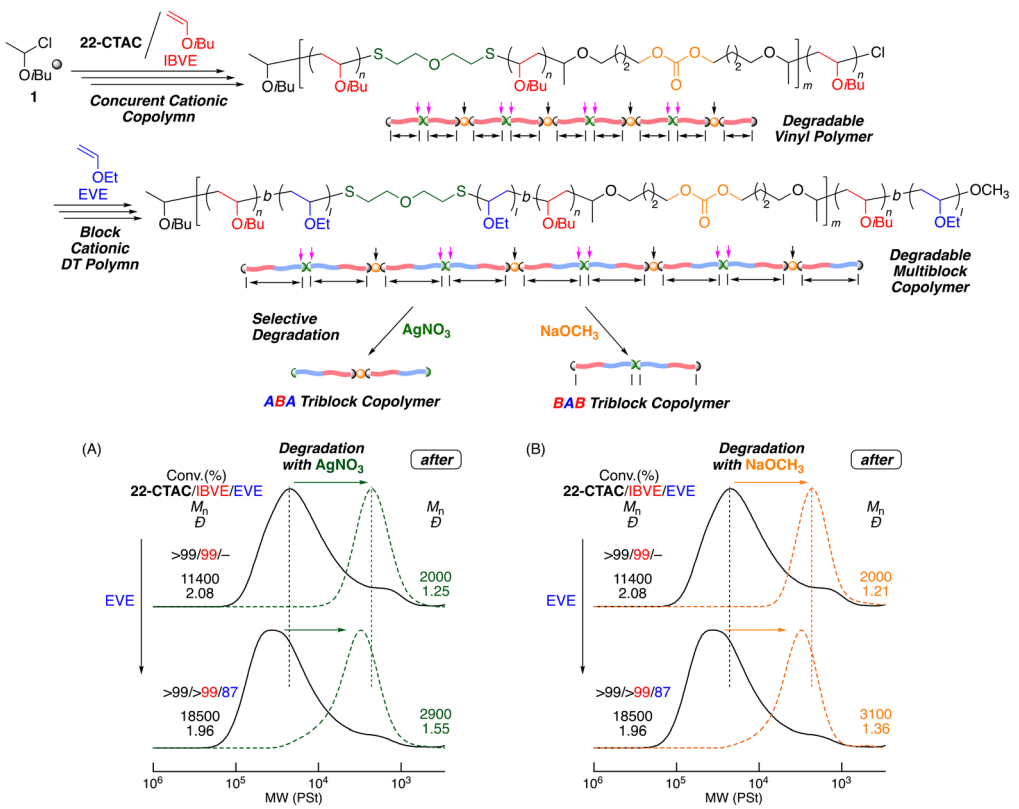

Fig. 9 One-pot synthesis of dual-degradable multiblock copolymers linked by thioacetal bonds and degradation with $AgNO_3$ (A) and $NaOCH_3$ (B) into the triblock copolymers: $[IBVE]_0/[EVE]_{add}/[\mathbf{22\text{-}CTA}]_0/[\mathbf{1}]_0/[ZnCl_2]_0$ = 2000/2000/200/20/4.0 mM in CH_2Cl_2/*n*-hexane/Et_2O (20/10/10) at −40 °C. $[Thioacetal\ unit]_0/[AgNO_3]_0$ = 5.0/50 mM in THF/H_2O at 20 °C. $[Carbonate]_0/[NaOCH_3]_0$ = 5.0/50 mM in CH_3OH at 60 °C.

with carbonate bonds in the middle of the B-segment, whereas those obtained with $NaOCH_3$ were BAB triblock polymers with thioacetal bonds in the middle of the A-segment. These results indicated that the block copolymerization of different vinyl ethers using macrocyclic thioacetal carbonate enabled the one-pot synthesis of dual-degradable multiblock copolymers; ultimately, this resulted in the ABA and BAB triblock polymers by the selective orthogonal degradation.

Conclusions

The synthesis of dual-stimuli degradable poly(vinyl ether)s with thioacetal and carbonate bonds evenly distributed in the main chain was achieved by cationic DT copolymerization of vinyl ethers and the design of macrocyclic thioacetal carbonates; these were prepared by a cationic thiol–ene reaction between divinyl ether and dithiol containing carbonate bonds. The macrocyclic thioacetal carbonates underwent efficient ring-opening cationic polymerization to generate the main-chain thioacetal and carbonate bonds; here, the macrocyclic thioacetal carbonate served as dormant species for the cationic DT polymerization of the vinyl ethers to control the total and segmental molecular weights. The main-chain thioacetal and carbonate bonds were selectively degraded to low-molecular-weight products with narrow dispersities using acid and base catalysts, respectively. Furthermore, multiblock copolymers with dual degradability were synthesized by the one-time addition of the second monomer and were degraded into ABA and BAB triblock copolymers with different sequences by the orthogonal degradation. Furthermore, the carbonate bonds in macrocyclic thioacetal carbonate could be replaced with other cleavable bonds; this aspect will advance multi-degradable polymers and further contribute to the macromolecular design of sustainable polymer materials.

Author contributions

M. U., K. M., and M. K. designed the experiments. M. U. and K. M. conducted the experiments. M. U., K. M., and M. K. anaylzed the results. M. U. and M. K. prepared the manuscript.

Data availability

The data supporting this article have been included as part of the ESI.†

Conflicts of interest

There are no conflicts to declare.

Acknowledgements

This work was supported by a JSPS KAKENHI Grant-in-Aid for Scientific Research (C) (no. JP22K05209) for M. U. and for Scientific Research (A) (no. JP22H00333 and JP25H00894) for M. K., a JST CREST (no. JPMJCR22L2) for M. U., and a project (JPNP18016) commissioned by the New Energy and Industrial Technology Development Organization (NEDO). The authors would like to thank Hironobu Watanabe and Chihiro Homma for fruitful discussions and valuable comments on this research.

References

1 J. R. Jambeck, R. Geyer, C. Wilcox, T. R. Siegler, M. Perryman, A. Andrady, R. Narayan and K. L. Law, *Science*, 2015, **347**, 768–771.
2 R. Geyer, J. R. Jambeck and K. L. Law, *Sci. Adv.*, 2017, **3**, e1700782.
3 A. Chamas, H. Moon, J. Zheng, Y. Qiu, T. Tabassum, J. H. Jang, M. Abu-Omar, S. L. Scott and S. Suh, *ACS Sustainable Chem. Eng.*, 2020, **8**, 3494–3511.
4 G.-X. Wang, D. Huang, J.-H. Ji, C. Völker and F. R. Wurm, *Adv. Sci.*, 2020, **8**, 2001121.
5 D. E. Fagnani, J. L. Tami, G. Copley, M. N. Clemons, Y. D. Y. L. Getzler and A. J. McNeil, *ACS Macro Lett.*, 2021, **10**, 41–53.
6 S. M. Clouthier, J. Li, J. Tanaka and W. You, *Polym. Chem.*, 2024, **15**, 17–21.
7 C.-C. Chang and T. Emrick, *Macromolecules*, 2014, **47**, 1344–1350.
8 K. Saito, F. Eisenreich and Ž. Tomović, *Macromolecules*, 2024, **57**, 8690–8697.
9 V. Delplace and J. Nicolas, *Nat. Chem.*, 2015, **7**, 771–784.
10 J. Pan, X. Ai, C. Ma and G. Zhang, *Acc. Chem. Res.*, 2022, **55**, 1586–1598.
11 J. Zheng, Z. M. Png, X. C. N. Quek, X. J. Loh and Z. Li, *Green Chem.*, 2023, **25**, 8903–8934.
12 C. Lefay and Y. Guillaneuf, *Prog. Polym. Sci.*, 2023, **147**, 101764.
13 L. Wu, B. Rondon, S. Dym, W. Wang, K. Chen and J. Niu, *Prog. Polym. Sci.*, 2023, **145**, 101736.
14 M. Kamigaito, *Bull. Chem. Soc. Jpn.*, 2024, **97**, uoae069.
15 S. Tang, F. W. Seidel and K. Nozaki, *Angew. Chem., Int. Ed.*, 2021, **60**, 26506–26510.
16 M. Mizutani, K. Satoh and M. Kamigaito, *J. Am. Chem. Soc.*, 2010, **132**, 7498–7507.
17 T. Kimura, K. Kuroda, H. Kubota and M. Ouchi, *ACS Macro Lett.*, 2021, **10**, 1535–1539.
18 J. B. Garrison, R. W. Hughes and B. S. Sumerlin, *ACS Macro Lett.*, 2022, **11**, 441–446.
19 S. Yamamoto, T. Kubo and K. Satoh, *J. Polym. Sci.*, 2022, **60**, 3435–3446.
20 H. S. Wang, N. P. Truong, Z. Pei, M. L. Coote and A. Anastasaki, *J. Am. Chem. Soc.*, 2022, **144**, 4678–4684.

21 S. Oh and E. E. Stache, *J. Am. Chem. Soc.*, 2022, **144**, 5745–5749.
22 L. H. Kugelmass, C. Tagnon and E. E. Stache, *J. Am. Chem. Soc.*, 2023, **145**, 16090–16097.
23 W. J. Bailey, *Polym. J.*, 1985, **17**, 85–95.
24 F. Sanda and T. Endo, *J. Polym. Sci., Part A: Polym. Chem.*, 2001, **39**, 265–276.
25 A. Tardy, J. Nicolas, D. Gigmes, C. Lefay and Y. Guillaneuf, *Chem. Rev.*, 2017, **117**, 1319–1406.
26 T. Pesenti and J. Nicolas, *ACS Macro Lett.*, 2020, **9**, 1812–1835.
27 A. W. Jackson, *Polym. Chem.*, 2020, **11**, 3525–3545.
28 Y. Deng, F. Mehner and J. Gaitzsch, *Macromol. Rapid Commun.*, 2023, **44**, e2200941.
29 W. J. Bailey, Z. Ni and S.-R. Wu, *Macromolecules*, 1982, **15**, 711–714.
30 T. Zeng, W. You, G. Chen, X. Nie, Z. Zhang, L. Xia, C. Hong, C. Chen and Y. You, *iScience*, 2020, **23**, 100904.
31 A. Tardy, N. Gil, C. M. Plummer, C. Zhu, S. Harrisson, D. Siri, J. Nicolas, D. Gigmes, Y. Guillaneuf and C. Lefay, *Polym. Chem.*, 2020, **11**, 7159–7169.
32 R. A. Evans, G. Moad, E. Rizzardo and S. H. Thang, *Macromolecules*, 1994, **27**, 7935–7937.
33 R. A. Evans and E. Rizzardo, *Macromolecules*, 1996, **29**, 6983–6989.
34 J. M. Paulusse, R. J. Amir, R. A. Evans and C. J. Hawker, *J. Am. Chem. Soc.*, 2009, **131**, 9805–9812.
35 H. Huang, B. Sun, Y. Huang and J. Niu, *J. Am. Chem. Soc.*, 2018, **140**, 10402–10406.
36 N. M. Bingham and P. J. Roth, *Chem. Commun.*, 2019, **55**, 55–58.
37 R. A. Smith, G. Fu, O. McAteer, M. Xu and W. R. Gutekunst, *J. Am. Chem. Soc.*, 2019, **141**, 1446–1451.
38 G. R. Kiel, D. J. Lundberg, E. Prince, K. E. L. Husted, A. M. Johnson, V. Lensch, S. Li, P. Shieh and J. A. Johnson, *J. Am. Chem. Soc.*, 2022, **144**, 12979–12988.
39 O. Ivanchenko, S. Mazières, S. Harrisson and M. Destarac, *Polym. Chem.*, 2022, **13**, 5525–5529.
40 R. Kamiki, T. Kubo and K. Satoh, *Macromol. Rapid Commun.*, 2023, **44**, e2200537.
41 M. Pięta, V. B. Purohit, P. Paneth, J. Pietrasik, L. Li and C. M. Plummer, *Polym. Chem.*, 2023, **14**, 3872–3880.
42 A. Kazama and Y. Kohsaka, *Polym. Chem.*, 2019, **10**, 2764–2768.
43 X. Y. Oh, Y. Ge and A. Goto, *Chem. Sci.*, 2021, **12**, 13546–13556.
44 A. Kanazawa, S. Kanaoka and S. Aoshima, *J. Am. Chem. Soc.*, 2013, **135**, 9330–9333.
45 T. Shirouchi, A. Kanazawa, S. Kanaoka and S. Aoshima, *Macromolecules*, 2016, **49**, 7184–7195.
46 A. Kanazawa and S. Aoshima, *Macromolecules*, 2020, **53**, 5255–5265.
47 K. Maruyama, A. Kanazawa and S. Aoshima, *Macromolecules*, 2022, **55**, 4034–4045.
48 A. Katto, S. Aoshima and A. Kanazawa, *Macromolecules*, 2024, **57**, 6255–6266.
49 T. Shen, K. Chen, Y. Chen and J. Ling, *Macromol. Rapid Commun.*, 2023, **44**, e2300099.
50 Y. Takahashi, A. Kanazawa and S. Aoshima, *Macromolecules*, 2023, **56**, 4198–4207.
51 A. E. Neitzel, L. Barreda, J. T. Trotta, G. W. Fahnhorst, T. J. Haversang, T. R. Hoye, B. P. Fors and M. A. Hillmyer, *Polym. Chem.*, 2019, **10**, 4573–4583.
52 H. Watanabe and M. Kamigaito, *J. Am. Chem. Soc.*, 2023, **145**, 10948–10953.
53 O. Ivanchenko and M. Destarac, *ACS Macro Lett.*, 2024, **13**, 47–51.
54 Y. Ishido, R. Aburaki, S. Kanaoka and S. Aoshima, *Macromolecules*, 2010, **43**, 3141–3144.
55 Y. Ishido, A. Kanazawa, S. Kanaoka and S. Aoshima, *Macromolecules*, 2012, **45**, 4060–4068.
56 M. Kawamura, A. Kanazawa, S. Kanaoka and S. Aoshima, *Polym. Chem.*, 2015, **6**, 4102–4108.
57 T. Nara, A. Kanazawa and S. Aoshima, *Macromolecules*, 2022, **55**, 6852–6859.
58 K. Kuroda and M. Ouchi, *Angew. Chem., Int. Ed.*, 2024, **63**, e202316875.
59 M. Uchiyama, M. Imai and M. Kamigaito, *Polym. J.*, 2024, **56**, 359–368.
60 Y. Chen, C. Yue, B. An, S. Liu, L. Zhou, C.-L. Ji and Y. Li, *Macromolecules*, 2024, **57**, 4918–4925.
61 F. Kawai, *Appl. Microbiol. Biotechnol.*, 1993, **39**, 382–385.
62 T. Hayashi, M. Mukouyama, K. Sakano and Y. Tani, *Appl. Environ. Microbiol.*, 1993, **59**, 1555–1559.
63 S. M. Barbon, M. C. D. Carter, L. Yin, C. M. Whaley, V. C. Albright and R. E. Tecklenburg, *Macromol. Rapid Commun.*, 2022, **43**, e2100773.
64 M. Uchiyama, K. Satoh and M. Kamigaito, *Angew. Chem., Int. Ed.*, 2015, **54**, 1924–1928.
65 M. Uchiyama, K. Satoh and M. Kamigaito, *Macromolecules*, 2015, **48**, 5533–5542.
66 M. Uchiyama, K. Satoh and M. Kamigaito, *Polym. Chem.*, 2016, **7**, 1387–1396.
67 M. Kamigaito, K. Satoh and M. Uchiyama, *J. Polym. Sci., Part A: Polym. Chem.*, 2019, **57**, 243–254.
68 M. Kamigaito and M. Sawamoto, *Macromolecules*, 2020, **53**, 6749–6753.
69 M. Uchiyama, K. Satoh and M. Kamigaito, in *RAFT Polymerization: Methods, Synthesis, and Applications*, ed. G. Moad and E. Rizzardo, Wiley-VCH GmbH, Weinheim, 2021, pp. 1171–1194.
70 M. Uchiyama, K. Satoh and M. Kamigaito, *Prog. Polym. Sci.*, 2022, **124**, 101485.
71 M. Uchiyama, M. Sakaguchi, K. Satoh and M. Kamigaito, *Chin. J. Polym. Sci.*, 2019, **37**, 851–857.
72 M. Uchiyama, M. Osumi, K. Satoh and M. Kamigaito, *Macromol. Rapid Commun.*, 2021, **42**, 2100192.
73 M. Matsuda, M. Uchiyama, Y. Itabashi, K. Ohkubo and M. Kamigaito, *Polym. Chem.*, 2022, **13**, 1031–1039.
74 M. Uchiyama, K. Satoh and M. Kamigaito, *ACS Macro Lett.*, 2016, **5**, 1157–1161.

75 M. Uchiyama, K. Satoh and M. Kamigaito, *Giant*, 2021, **5**, 100047.
76 M. Uchiyama, D. Watanabe, Y. Tanaka, K. Satoh and M. Kamigaito, *J. Am. Chem. Soc.*, 2022, **144**, 10429–10437.
77 R. J. Sifri, A. J. Kennedy and B. P. Fors, *Polym. Chem.*, 2020, **11**, 6499–6504.
78 P. C. Knutson, A. J. Teator, T. P. Varner, C. T. Kozuszek, P. E. Jacky and F. A. Leibfarth, *J. Am. Chem. Soc.*, 2021, **143**, 16388–16393.
79 Z. Yang, W. Xiao, X. Zhang and S. Liao, *Polym. Chem.*, 2022, **13**, 2776–2781.
80 M. Uchiyama, Y. Murakami, K. Satoh and M. Kamigaito, *Angew. Chem., Int. Ed.*, 2023, **62**, e202215021.
81 M. Uchiyama, M. Osumi, K. Satoh and M. Kamigaito, *Angew. Chem., Int. Ed.*, 2020, **59**, 6832–6838.
82 T. H. Fife and L. K. Jao, *J. Am. Chem. Soc.*, 1969, **91**, 4217–4220.
83 J. L. Jensen and W. P. Jencks, *J. Am. Chem. Soc.*, 1979, **101**, 1476–1488.
84 D. P. N. Satchell, *Chem. Soc. Rev.*, 1977, **6**, 345–371.
85 D. P. N. Satchell and R. S. Satchell, *Chem. Soc. Rev.*, 1990, **19**, 55–81.